Universality, the QCD critical and tricritical point, and the quark number susceptibility

Yoshitaka Hatta
Department of Physics, Kyoto University, Kyoto 606-8502, Japan
and The Institute of Physical and Chemical Research (RIKEN), Wako, Saitama 351-0198, Japan

Takashi Ikeda
RIKEN BNL Research Center, Brookhaven National Laboratory, Upton, New York 11973-5000
(Received 23 October 2002; published 31 January 2003)

The quark number susceptibility near the QCD critical end point (CEP), the tricritical point (TCP) and the $O(4)$ critical line at finite temperature and quark chemical potential are investigated. Based on the universality argument and numerical model calculations we propose the possibility that the hidden tricritical point strongly affects the critical phenomena around the critical end-point. We make a semiquantitative study of the quark number susceptibility near CEP or TCP for several quark masses on the basis of the Cornwall-Jackiw-Tomboulis potential for QCD in the improved-ladder approximation. The results show that the susceptibility is enhanced in a wide region around the CEP, inside which the critical exponent gradually changes from that of the CEP to that of the TCP, indicating a crossover of different universality classes.

DOI: 10.1103/PhysRevD.67.014028 PACS number(s): 12.38.−t, 05.70.Jk, 11.15.Tk, 25.75.−q

I. INTRODUCTION

The vacuum of quantum chromodynamics (QCD) is believed to undergo a phase transition to the quark-gluon plasma (QGP) at high temperature T and/or at high quark chemical potential μ. Such a new state of matter is expected to be produced in on-going heavy-ion collision experiments at the BNL Relativistic Heavy-Ion Collider (RHIC) and in the future Large Hadron Collider (LHC) [1].

The phase transition of the hadronic matter to the QGP at finite T with $\mu=0$ has been studied extensively on the lattice. In particular, the chiral phase transition is likely to be of second order for QCD with two massless quarks. Also, the static critical behavior is expected to fall into the universality class of the $O(4)$ spin model in three dimensions [2]. In nature, the light quarks have small but finite masses and the second order transition becomes a smooth crossover.

The study of the QCD phase transition with finite μ has been retarded because reliable lattice simulations have not been available so far due to the severe fermion sign problem. Nevertheless, there is growing evidence that the phase diagram of QCD with massless two-flavors has a tricritical point (TCP, Fig. 1, point P) at which a line of critical points [the $O(4)$ line] at lower μ's turns into a first-order phase transition line at higher μ's. The existence of the TCP was in fact suggested in various calculations based on effective theories of QCD [3–10]. If the u- and d-quark masses are increased from zero, a line of critical points (the wing critical line) emerges from the TCP and the point which corresponds to the physical quark mass m_{phys} is called the QCD critical end point (CEP, Fig. 1, point E), because this is the point where the first-order phase transition line terminates. Indeed, some evidence of the existence of the CEP was shown recently in a lattice QCD simulation with 2+1 flavors by Fodor and Katz [11]. In this paper we assume that CEP exists in the phase diagram of QCD.[1]

Second-order phase transitions are characterized by the long-wavelength fluctuations of the order parameter. In the case of the CEP, it is the sigma (σ) field. Then, it is expected that the fluctuations of the sigma field will be reflected in the event-by-event fluctuation of pion (π) observables due to the the $\pi-\sigma$ coupling. Based on this observation, possible observable signals associated with the CEP have been studied in detail in relation to the relativistic heavy-ion collision experiments [12–14].

The purpose of this paper is to point out that the anomaly near the CEP is not pointlike but has much richer structure. Our starting point is a simple question: ''How large is the critical region?'' The critical region is defined as the region where the mean field theory (or the Landau theory) of phase transitions breaks down and the true nontrivial critical exponents can be seen. Usually, one expects that the critical region is surrounded by the mean field region and the critical exponents change from the nontrivial values to the mean field values as one goes away from the critical point. One might argue that this question is only of academic interest because the nontrivial exponents and the mean field exponents are numerically not so different and probably experiments cannot distinguish them. (This observation is the basis of [12].) However, as we will see, pursuing this question leads to an important notion that may shed light on certain results of both heavy-ion collision experiments and future lattice simulations at finite chemical potentials.

There is a well-known criterion which estimates the size of the critical region, the Ginzburg criterion [15]. It shows that if the singular part of the thermodynamic potential Ω

[1]Accordingly, we fix the strange quark mass to its physical value. Below ''the quark mass'' means the u, d current quark masses which we consider as variable parameters.

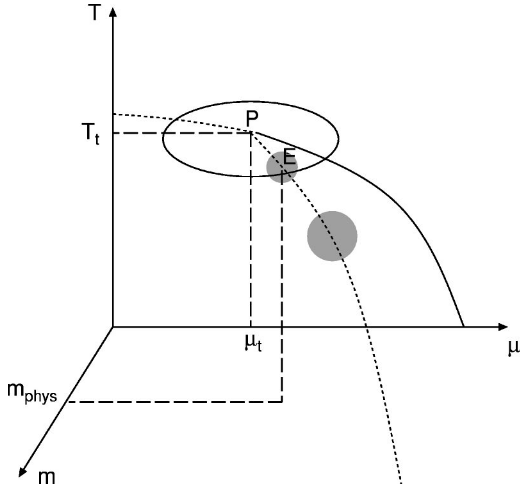

FIG. 1. The phase diagram of QCD in the (T,μ,m) space. Point P is the tricritical point (TCP) of the massless theory and point E is the critical end point (CEP) of the real world. The dotted lines represent the second-order phase transition and the solid line represents the first-order phase transition.

(the Landau-Ginzburg potential) for a certain second-order phase transition is given by

$$\Omega|_{singular}=c(\nabla\phi)^2+at\phi^2+b\phi^4, \tag{1.1}$$

where ϕ is the order parameter and $t\equiv(T-T_c)/T_c$ is the reduced temperature (T_c is the critical temperature in the mean field approximation), the critical region is estimated to be

$$|t|\sim\frac{T_c^2b^2}{ac^3}. \tag{1.2}$$

At first sight, this criterion seems useless because we do not know the coefficients appearing in Eq. (1.1) for the CEP.[2] However, in the next section we will derive a bound to the size of the critical region. In fact, there is a reason to expect that the critical region of the CEP is *small*. This is because the QCD critical end point is a descendant of the tricritical point of the massless theory.

This observation led us to study the critical phenomena of both the CEP and TCP simultaneously and their possible correlations. We make both qualitative and quantitative analyses of the physics near the TCP and CEP with particular emphasis on the (singular) behavior of the quark number susceptibility χ_q defined by

$$\chi_q=-\frac{1}{V}\frac{\partial^2\Omega}{\partial\mu^2}, \tag{1.3}$$

where $\Omega(T,\mu)$ is the thermodynamic potential and V is the volume of the system. χ_q is a response of the quark number density to the variation of the quark chemical potential and is one of the key quantities characterizing the phase change from the hadronic matter to QGP [18–21,45]. The lattice data show that, at $\mu=0$, χ_q increases rapidly but smoothly near the critical temperature [22–24]. On the other hand, the universality argument predicts that it diverges at both the TCP and CEP with certain critical exponents. Therefore, it would be important to study its critical behavior with and without the quark masses to see whether or not it can provide a new way of detecting the TCP or CEP on the lattice as well as in the heavy-ion collision experiments.

In addition to χ_q, we occasionally mention the singular behavior of the specific heat C and the chiral susceptibility χ_{ch} defined as

$$C=-\frac{T}{V}\frac{\partial^2\Omega}{\partial T^2}, \tag{1.4}$$

$$\chi_{ch}=\frac{1}{V}\frac{\partial^2\Omega}{\partial m^2}. \tag{1.5}$$

From the viewpoint of critical phenomena, χ_q and C are essentially the same near the TCP and CEP while χ_{ch} is different from χ_q near the TCP and only slightly different near the CEP in the sense that will be clarified below.

In Sec. II, we make a general analysis of the interplay between TCP and CEP in the small quark mass limit based on the universality argument. After determining the relative locations of the TCP and CEP in the phase diagram as functions of the quark mass, we construct the Landau-Ginzburg potential for the CEP to determine the singular behavior of susceptibilities both in and beyond the mean field approximation. It turns out that the smallness of the quark mass gives a bound to the growth of the critical region, turning our attention to the tricritical point. Then we discuss a possible crossover from the tricritical universality class to the Ising universality class.

The universality argument is so general that it gives no quantitative results. In order to reinforce the ideas given in Sec. II, in Sec. III we show the results of the numerical calculation on a model, the Cornwall-Jackiw-Tomboulis (CJT) potential for QCD [25] in the improved-ladder approximation [10,26]. We will find how well the numerical results match with the qualitative predictions of the universality argument, demonstrating the power of universality. In particular, we obsere some indication of the effect of the TCP on the QCD phase diagram even with a reasonable value of the quark mass. Section IV is devoted to conclusions.

[2]The size of the critical region depends on the microscopic dynamics and universality tells nothing about it. A clear example is the λ transition of liquid helium and the superconducting transition of metals. Although they belong to the same universality class [the $O(2)$ spin model], their critical regions are very different; $|t|\sim0.3$ for the λ point and $|t|\sim10^{-15}$ for conventional (type-I) superconductors. Just for reference, we note that for typical liquid-gas phase transitions which belong to the same universality class as the phase transition at the CEP, $|t|\sim10^{-2}$ [16]. (Corrections to the scaling [17] are not negligible until one reaches $|t|\sim10^{-4}$.)

A brief description of the model is given in Appendix A. In Appendix B, we discuss, for completeness, how χ_q behaves along the $O(4)$ line based on the universality argument. We will see that the monotonic increase so far observed on the lattice is a property only at $\mu=0$.

II. UNIVERSALITY ARGUMENTS

Universality is such a strong notion of modern physics [27] that its applicability ranges from phase transitions in ordinary liquids to thermal phase transitions of relativistic quantum field theories. In this section we study the critical phenomena near the CEP and TCP based on the universality argument. We will see that a lot of general information can be extracted by the universality argument alone without mentioning any complexities of the strong interaction.

A. The QCD critical end-point

It was suggested theoretically [4,5,8,10] and found on the lattice [11] that QCD has the CEP at finite temperature T_c and baryon chemical potential μ_c (Fig. 1, point E). At the critical end point, only the σ field becomes massless and the universality class of this phase transition is considered to be the same as that of the liquid-gas phase transition, or equivalently, that of the three-dimensional Ising model.[3]

In order to exploit the power of universality to investigate the singular behavior of various quantities, we consider the mapping of the (t_I,h_I) axes of the Ising model (t_I is the reduced temperature and h_I is the reduced magnetic field) onto the (T,μ,m) space (m is the light quark mass divided by the typical scale of the problem such as T_c). This can be achieved by considering the tricritical point (TCP) at $(T,\mu,m)=(T_t,\mu_t,0)$ (Fig. 1, point P). Below we explicitly construct the Landau-Ginzburg potential for the CEP starting from the general theory of tricritical points [29] and discuss associated universal behaviors.

Near the TCP, the long-wavelength physics of the system can be described by the thermodynamic potential expanded up to the sixth order in the order parameter field (the sigma field) σ,

$$\Omega_{MF}=\Omega_0-m\sigma+\frac{a}{2}\sigma^2+\frac{b}{4}\sigma^4+\frac{c}{6}\sigma^6, \tag{2.1}$$

where Ω_0 is the contribution from short-wavelength degrees of freedom irrelevant to the study of critical phenomena.

At the TCP, $a=b=m=0$. Assuming that a and b are analytic in T and μ and that $c>0$ is approximately constant near the tricritical point, we expand them as follows [30]:

$$a(T,\mu)=C_a(T-T_t)+D_a(\mu-\mu_t),$$
$$b(T,\mu)=C_b(T-T_t)+D_b(\mu-\mu_t), \tag{2.2}$$

where we have neglected higher-order terms in the deviation from the tricritical point. $C_a>0$ and $D_a>0$ are related such that the line $a(T,\mu)=0$ is tangential to the first-order phase transition curve at the TCP. b is positive for $T-T_t>0$ ($\mu<\mu_t$) on the $a=0$ line, which leads to the condition

$$C_bD_a-C_aD_b>0. \tag{2.3}$$

These conditions come from the geometry of the phase diagram, namely, the fact that there is a line of (bi)critical points at $T>T_t$, $\mu<\mu_t$. We do not know the actual values of these coefficients. But we need not know them for the present purpose.

If we increase m from zero, at some point $(T_c(m),\mu_c(m))$ in the (T,μ) plane two minima and a maximum of the potential coalesce. This is the critical end point. There the sigma field acquires a nonzero expectation value σ_0 which is determined by the following equations [in this section we exclusively consider the small m limit and leave only the leading terms in m]:

$$\Omega'(T_c(m),\mu_c(m),\sigma_0)=-m+a_m\sigma_0+b_m\sigma_0^3+c\sigma_0^5=0,$$
$$\Omega''(T_c(m),\mu_c(m),\sigma_0)=a_m+3b_m\sigma_0^2+5c\sigma_0^4=0,$$
$$\Omega'''(T_c(m),\mu_c(m),\sigma_0)=6b_m\sigma_0+20c\sigma_0^3=0, \tag{2.4}$$

where $a_m\equiv a(T_c(m),\mu_c(m))$ and $b_m\equiv(T_c(m),\mu_c(m))$. The solution is

$$a_m=\frac{9b_m^2}{20c},$$
$$-b_m=\frac{5}{54^{1/5}}c^{3/5}m^{2/5},$$
$$\sigma_0=\sqrt{\frac{-3b_m}{10c}}. \tag{2.5}$$

Using Eqs. (2.2) and (2.5) we can locate the critical end point for small m:

$$T_c(m)-T_t=-\frac{45D_ac^{1/5}}{4(54)^{2/5}(C_bD_a-C_aD_b)}m^{2/5}+O(m^{4/5}),$$
$$\mu_c(m)-\mu_t=\frac{5C_ac^{3/5}}{(54)^{1/5}(C_bD_a-C_aD_b)}m^{2/5}+O(m^{4/5}). \tag{2.6}$$

Thus, as we increase the quark mass m, the critical temperature decreases and the critical chemical potential increases at

[3]This is not obvious *a priori* and requires explanation. As we shall see below, the phase transition at the end point is characterized by the one-component order parameter $\hat{\sigma}$. The effective Landau-Ginzburg potential contains odd powers of $\hat{\sigma}$, which break the $\hat{\sigma}\to-\hat{\sigma}$ symmetry of the Ising model. This is the same situation as the liquid-gas phase transition. Theoretically, the usual renormalization group argument should be reconsidered in the presence of the asymmetry [28]. Although there are some subtleties about this problem, *experimentally* it is clear that the liquid-gas phase transition and the 3D Ising model belong to the same universality class.

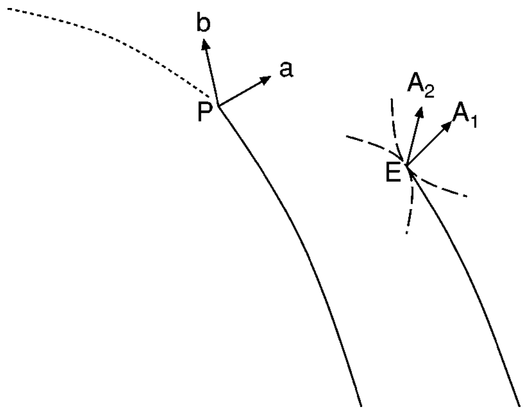

FIG. 2. The mapping of the Ising model axes onto the (T,μ) plane. The solid lines represent the first-order phase transition (the coexisting line). The dashed lines separate regions with different exponents.

least for small m (Fig. 1). Expanding $\Omega(T,\mu,\sigma)$ around $(T_c(m),\mu_c(m),\sigma_0)$ we obtain the Landau-Ginzburg potential with the new order parameter $\hat{\sigma}\equiv\sigma-\sigma_0$:

$$\Omega_{MF}(T,\mu,\hat{\sigma})=\Omega_{MF}(T_c(m),\mu_c(m),\sigma_0)+A_1\hat{\sigma}+A_2\hat{\sigma}^2+A_3\hat{\sigma}^3+A_4\hat{\sigma}^4, \tag{2.7}$$

where

$$\begin{aligned}A_1&=(C_a\sigma_0+C_b\sigma_0^3)[T-T_c(m)]+(D_a\sigma_0+D_b\sigma_0^3)\times[\mu-\mu_c(m)],\\ A_2&=(C_a+3C_b\sigma_0^2)[T-T_c(m)]+(D_a+3D_b\sigma_0^2)\times[\mu-\mu_c(m)],\\ A_3&=C_b(T-T_c(m))+D_b[\mu-\mu_c(m)],\\ A_4&=\frac{-b_m}{2}.\end{aligned} \tag{2.8}$$

$A_i(i=1,2,3)$ vanish at the critical point whereas A_4 does not, indicating that $(T_c(m),\mu_c(m))$ is an ordinary (bi)critical point as stated above.

Looking at Eqs. (2.7) and (2.8), we immediately notice two important things. First, A_2 is a linear combination of $T-T_c(m)$ and $\mu-\mu_c(m)$. This means that T and μ are equivalent thermodynamic variables in the sense of Griffiths and Wheeler [31] and that A_2 is the temperaturelike scaling field which corresponds to t_I of the Ising model. Second, A_1, rather than the quark mass plays the role of the "external field" which is conjugate to the new order parameter. Thus it can be identified as the magnetic fieldlike scaling field h_I. Indeed, it is easy to show that, on the line $A_1=0$, A_2 and A_3 are positive for $T>T_c(m)$ [or $\mu<\mu_c(m)$] and negative for $T<T_c(m)$ (or $\mu<\mu_c(m)$) and this line is asymptotically parallel to the first order phase transition line at the critical end point. See Fig. 2.

Now we can discuss the critical behavior of susceptibilities; the quark number susceptibility χ_q, the specific heat C, and the chiral susceptibility χ_{ch}. In the mean field approximation, the equilibrium value of $\hat{\sigma}$ is determined by the first- and fourth-order terms of Eq. (2.7) in the small mass limit. Then we obtain, for paths asymptotically not parallel to the $A_1=0$ line, (the first order phase transition line)

$$\begin{aligned}\chi_q&\sim C\sim m^{2/15}|g-g_c|^{-\epsilon},\\ \chi_{ch}&\sim m^{-16/15}|g-g_c|^{-\epsilon},\end{aligned} \tag{2.9}$$

where $\epsilon\equiv\gamma/\beta\delta=\frac{2}{3}$. $|g-g_c|$ denotes the distance from the CEP in some units. For the path asymptotically parallel to the $A_1=0$ line, the exponent is $\gamma=1>\epsilon$. Note that, although the critical exponents are the same, the *amplitude* of the chiral susceptibility is enhanced whereas that of the quark number susceptibility is suppressed by factors of m.

Inside the critical region, where the mean field theory breaks down, $\Omega|_{singular}$ does not admit a simple expansion with smooth coefficients. Equation (2.7) should be regarded as the saddle point approximation to the following functional integral:

$$\Omega(T,\mu,\hat{\sigma})=-\frac{T}{V}\ln\int[d\sigma']\exp\left(-\frac{1}{T}\int d^3\mathbf{r}H_{eff}(\mathbf{r})\right), \tag{2.10}$$

where H_{eff} is the Landau-Ginzburg-Wilson Hamiltonian

$$H_{eff}=A_0'(\boldsymbol{\nabla}\sigma')^2+A_1'\sigma'+A_2'\sigma'^2+A_3'\sigma'^3+A_4'\sigma'^4. \tag{2.11}$$

$A_i'(i=1$–$4)$ are in general different from A_i due to fluctuations. However, we expect that the differences between A_i' and A_i are of the higher order in m.[4] Note the appearance of the kinetic term. The sigma field is no longer a constant beyond the mean field approximation. The potential (2.10) will eventually lead to the *scaling equation of state* [32] written in terms of the scaling fields A_1 and A_2 (the revised scaling [33]). Because T, μ, and m participate in the magnetic-field-like scaling field, we obtain, very schematically, the most singular part[5]

$$\chi_q\sim\frac{\partial^2\Omega}{\partial\mu^2}\sim m^{2/5}\frac{\partial^2\Omega}{\partial A_1^2}\sim m^{2/5}\langle\sigma'\sigma'\rangle,$$

[4]The coefficients are further affected by the change of integration variables. These degrees of freedom can eliminate A_3', but do not change $A_{1,2}'$ in the leading order. In fact, only the direction of A_1' is important for discussing the behaviors of quantities considered here (i.e., second derivatives of Ω in directions parallel to the T, μ, and m axes) [31,33].

[5]In calculating χ_{ch}, dominant contribution to dA_1/dm comes from $\sigma_0 d(T-T_c(m))/dm$ rather than $d\sigma_0/dm[T-T_c(m)]$. The latter term, being proportional to $T-T_c(m)$, behaves as a correction to the scaling. Also, if the derivative acts on A_2, we get $\langle\sigma'^2\sigma'^2\rangle\sim|g-g_c|^{-\alpha/\beta\delta}$, which is less singular than the magnetic susceptibility.

$$C\sim\frac{\partial^2\Omega}{\partial T^2}\sim m^{2/5}\frac{\partial^2\Omega}{\partial A_1^2}\sim m^{2/5}\langle\sigma'\sigma'\rangle,$$

$$\chi_{ch}\sim\frac{\partial^2\Omega}{\partial m^2}\sim m^{-4/5}\frac{\partial^2\Omega}{\partial A_1^2}\sim m^{-4/5}\langle\sigma'\sigma'\rangle,$$

$$\langle\sigma'\sigma'\rangle\sim|g-g_c|^{-\epsilon}, \tag{2.12}$$

where $|g-g_c|$ is the distance from the critical end point in some units. $\epsilon\equiv\gamma/\beta\delta\approx0.8$ for any direction which makes an angle with the $A_1=0$ line at the critical end point. For the path asymptotically parallel to that line, the exponent is $\gamma\sim1.2>\epsilon$. (These values are taken from the 3D Ising model.)

Having discussed the singular behavior of susceptibilities inside the critical region, however, we give a pessimistic result. Since we now have the Landau-Ginzburg potential for the CEP, we can discuss the size of the critical region. Recall that, according to the Ginzburg criterion (1.2), the radius of the critical region is proportional to the square of the coefficient of the quartic term. Other coefficients are quark mass independent in the leading order. Thus we obtain

$$|t|\sim A_4^2\sim m^{4/5}. \tag{2.13}$$

This gives a bound to the size of the critical region. It shrinks to zero as the quark mass decreases (see, Fig. 1). The physical reason behind this is that the coefficient of the quartic term is zero at the tricritical point and remains small near it.

Generally speaking, the critical point of a strongly interacting system has a large critical region [34]. Thus the size of the critical region of the CEP is subject to a competition between these opposite effects and the determination of it is a highly nontrivial problem. However, it seems to us that the above bound (2.13) is a compelling reason to expect that the critical region is "small."

If the critical region of the CEP is small, probably most of the fluctuations associated with the CEP come from the mean field region around the critical region.[6] The central point of this paper is that *if we consider the mean field region belonging to the CEP, we should also consider the mean field region belonging to the TCP*. The tricritical point has, so to speak, a "tricritical region" (see Fig. 1), which is a sphere or an ellipsoid in the (T,μ,m) space centered at $(T_t,\mu_t,0)$.[7] Then it is possible that *the tricritical region survives in the physical (T,μ) plane*. The magnitudes of the *u*-, *d*-quark masses are crucial to this. A more interesting possibility is that *the critical point is inside the tricritical region and a crossover of different universality classes occurs* (not to be confused with the crossover phase transition at lower chemical potentials). Namely, as we approach the CEP, the critical exponents gradually change from those of the tricritical point to those of the 3D Ising model *via* those of the CEP in the mean field approximation. (Note that the mean field exponents of a bicritical point are different from those of a tricritical point.) Indeed, such a kind of crossover was experimentally observed in an antiferromagnet dysprosium aluminum garnet long ago. The critical exponent β for the magnetization tends to change from the tricritical value ($\beta=1$) to the Ising model value ($\beta\simeq0.31$) as we go along the wing critical line [35].

Thus, through the consideration of the critical region, we have become aware of a possible interesting role played by the hidden tricritical point. Its critical phenomena are therefore worth studying and will be discussed in the next section.

B. The QCD tricritical point

Motivated by the above arguments, we now turn our attention back to the QCD tricritical point. Because the upper critical dimension of models described by Eq. (2.1) is 3, the origin of the coupling constant is an attractive IR fixed point. Correspondingly, universal behaviors associated with the tricritical point are well described by the mean field theory up to logarithmic corrections.[8]

Let us see how susceptibilities scale with respect to $|T-T_t|$, $|\mu-\mu_t|$ and m in the mean field approximation.

At $(T,\mu,m=0)$, straightforward calculations show that

$$\chi_q\sim|h-h_t|^{-\gamma_q},$$

$$\chi_{ch}\sim|h-h_t|^{-\gamma_{ch}}, \tag{2.14}$$

where $|h-h_t|$ is the distance (in some units) from the TCP in the (T,μ) plane. $\gamma_q=\frac{1}{2}$, $\gamma_{ch}=1$ for paths which are not asymptotically tangential to the first-order phase transition line.

At $(T,\mu,m\neq0)$, the expectation value of σ is given by the following equation:

$$m=a\sigma+b\sigma^3+\sigma^5. \tag{2.15}$$

Near (T_t,μ_t,m) where $a=b=0$, (note that this is the "nearest" point to the TCP in the phase diagram with a quark mass m) we can expand the solution up to the second order in a and b,

[6]It must be cautioned that the mean field region does not always exist. For example, it is known that there is no mean field region for the λ transition of liquid helium (the critical region is large, $|t|\sim0.3$). However, if the critical region is squeezed by an explicit parameter of the theory as in the present situation, it would be meaningful to discuss the mean field region belonging to the critical point. (We thank M. A. Stephanov for a discussion on this point.)

[7]Here we use the term "tricritical region" loosely for the region where any mean-field-like effects of the tricritical point on susceptibilities exist. This terminology is a bit misleading because there is no critical region for a tricritical point in the usual sense.

[8]This is why we neglected the pion degrees of freedom in Eq. (2.1). Mean field theory is truly universal in the sense that it does not depend on even the symmetry of the order parameter. However, the multiplicative logarithmic corrections to the scaling do depend on the symmetry of the order parameter.

$$\sigma = m^{1/5} - \frac{a}{5} m^{-3/5} - \frac{b}{5} m^{-1/5} + O(a^2 m^{-7/5}, b^2 m^{-3/5}, abm^{-1}). \tag{2.16}$$

Inserting Eq. (2.16) into Eq. (2.1) and differentiating with respect to μ twice, we get χ_q. Because of Eq. (2.2) the differentiation with respect to μ is replaced by the differentiation with respect to a and b. Extracting the most singular contribution, we obtain

$$\chi_q \sim \frac{\partial^2 \Omega[\sigma]}{\partial \mu^2}\Big|_{a=b=0} \sim m^{-2/5}. \tag{2.17}$$

Analogously,

$$\chi_{ch} \sim m^{-4/5}. \tag{2.18}$$

The divergence of χ_q is rather moderate in the mass direction, from which we expect that the quark number susceptibility may still be large even with nonzero quark masses. Indeed, from Eqs. (2.9) and (2.13) we can derive the m dependence of χ_q at the edge of the critical region

$$\chi_q \sim m^{2/15} |t|^{-2/3} \sim m^{2/15} (m^{4/5})^{-2/3} \sim m^{-2/5}. \tag{2.19}$$

Comparing with Eq. (2.17), we see that the m-dependence is exactly the same. There may or may not be a reason for this coincidence. In any case, this does show that the TCP is as important as the CEP at least in the small quark mass limit.

Starting from the simple Landau-Ginzburg potential, we have extracted a lot of physics near the CEP or TCP. These analyses show the power of universality as well as its limitations. For example, the universality argument does not tell us whether or not the effect of the TCP survives in the (T,μ) plane with the quark mass of, say, 5 MeV. In order to quantify the ideas given in this section, we must resort to a specific model. This is the subject of the next section.

III. NUMERICAL RESULTS

In this section, we numerically calculate the quark number susceptibility in the (T,μ) plane by using a model. As expected, the susceptibility diverges both at the critical and tricritical points. We also calculate the corresponding critical exponent. The results clearly demonstrate that the hidden tricritical point can affect the phase diagram with nonzero quark masses.

A. CJT effective potential and the chiral phase transition

As a model, we employ the Cornwall-Jackiw-Tomboulis (CJT) effective potential [25] for the two-flavor QCD in the improved-ladder approximation [10]. A brief description of the model is given in Appendix A. For more details, see [10].

At zero temperature and chemical potential, the effective potential V is given by

$$V[\Sigma] = -2\int \frac{d^4p}{(2\pi)^4} \ln\frac{\Sigma^2(p)+p^2}{p^2} - \frac{2}{3C_F}\int dp^2 \frac{1}{\dfrac{d}{dp^2}\dfrac{\overline{g}^2(p^2)}{p^2}} \left(\frac{d\Sigma(p)}{dp^2}\right), \tag{3.1}$$

where the gauge coupling constant $\overline{g}^2(p^2)$ and the dynamical quark mass function $\Sigma(p)$ are

$$\overline{g}^2(p^2) = \frac{2\pi^2 a}{\ln[(p^2+p_c^2)/\Lambda_{\rm QCD}{}^2]}, \tag{3.2}$$

$$\Sigma(p) = m_q \{\ln[(p^2+p_c^2)/\Lambda_{\rm QCD}{}^2]\}^{-a/2} + \frac{\sigma}{p^2+p_c^2}\{\ln[(p^2+p_c^2)/\Lambda_{\rm QCD}{}^2]\}^{a/2-1}. \tag{3.3}$$

p_c is a momentum scale which separates the infrared (nonperturbative) region from the ultraviolet (perturbative) region. $C_F = (N_c^2-1)/2N_c$ is the quadratic Casimir operator for the fundamental representation of the color SU(N_c) group and $a \equiv 24/(11N_c - 2N_f)$ (N_f is the number of active flavors.[9] σ is proportional to the renormalization group invariant chiral condensate $\langle\overline{q}q\rangle$ as $\sigma = 2\pi^2 a \langle\overline{q}q\rangle/3$ and m_q is the renormalization group invariant current quark mass.They are related to the scale dependent mass m_q^Λ and the scale dependent chiral condensate $\langle\overline{q}q\rangle^\Lambda$ through the perturbative renormalization group equation

$$\langle\overline{q}q\rangle = \frac{\langle\overline{q}q\rangle_\Lambda}{[\ln(\Lambda^2/\Lambda_{\rm QCD}{}^2)]^{a/2}}, \tag{3.4}$$

$$m_q = m_q^\Lambda [\ln(\Lambda^2/\Lambda_{\rm QCD}{}^2)]^{a/2}. \tag{3.5}$$

An overall factor ($N_f = 2$ times $N_c = 3$) is omitted in Eq. (3.1). The chiral condensate $\langle\overline{q}q\rangle$ and f_π are known to be insensitive to the infrared regularization parameter p_c [36]. Therefore we take $p_c^2/\Lambda_{\rm QCD}{}^2 = e^{0.1}$ and determine $\Lambda_{\rm QCD}$ to reproduce the pion decay constant $f_\pi = 93$ MeV in the Pagels-Stokar formula [37] in the chiral limit. We obtain $\Lambda_{\rm QCD} = 738$ MeV for $N_f = 2$ [10]. In the following calculations, we take $\Lambda = 1$ GeV in Eq. (3.5) and change the value of $m_q^{\Lambda=1\ \rm GeV}$. For simplicity, we abbreviate $m_q^{\Lambda=1\ \rm GeV}$ to m_q below.

At finite temperature and chemical potential,we use the imaginary time formalism [38], and make the replacement

[9]Although the potential is evaluated with $N_f = 2$, we take $N_f = 3$ in the gauge coupling (3.2). In this way we include the effect of the s quark only through the running of the coupling constant.

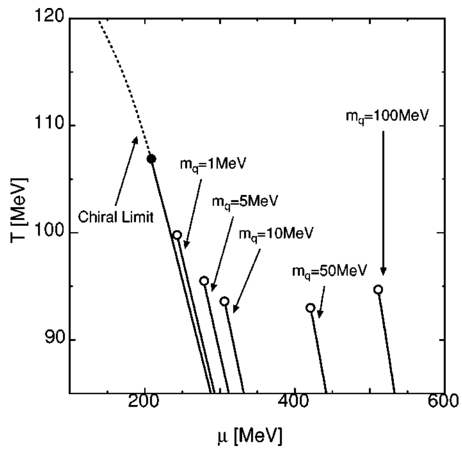

FIG. 3. The phase diagram with several quark masses. The quark masses are evaluated at the momentum scale 1 GeV. The solid and dotted lines represent the first-order and the second-order phase transitions, respectively. The filled circle is the tricritical point and open circles are the critical end points for different quark masses.

$$\int \frac{d^4p}{(2\pi)^4} f(\boldsymbol{p},p_4) \rightarrow T \sum_{n=-\infty}^{\infty} \int \frac{d^3\boldsymbol{p}}{(2\pi)^3} f(\boldsymbol{p},\omega_n+i\mu), \tag{3.6}$$

where $\omega_n=(2n+1)\pi T(n\in Z)$ is the Matsubara frequency for the quark.[10]

As a normalization, we define $\tilde{V}$ by subtracting the σ-independent part from V such that $\tilde{V}$ reduces to the value of the free quark gas when $\sigma=0$. See Appendix A.

We can study the chiral phase transition and the phase diagram by calculating $\tilde{V}[\sigma,m_q]$ at given T and μ and by searching the value of the chiral condensate σ_0 which minimizes the potential. The location of the first-order phase transition line is determined by finding a gap in σ_0. In the chiral limit, σ_0 goes to zero smoothly as the second-order phase transition line is approached from below. With finite quark masses, there is no distinct border between the symmetric and broken phases, and σ_0 remains finite at all temperatures and chemical potentials.

The phase diagram with several quark masses in the (T,μ) plane is shown in Fig. 3. The location of the tricritical point in the chiral limit is $T_t=107$ MeV and $\mu_t=209$ MeV. The open circles in Fig. 3 represent the critical end points for different quark masses. As shown in Fig. 4, the distance between the TCP and CEP approximately scales as $m_q^{2/5}$ up to $m_q\sim O(1)$ MeV, in agreement with Eq. (2.6). For larger masses, $m_q>10$ MeV, $T_c(m_q)$ does not change much while $\mu_c(m_q)$ keeps on increasing.

B. The quark number susceptibility around CEP and TCP

The quark number susceptibility χ_q is calculated from the normalized effective potential $\tilde{V}$ as

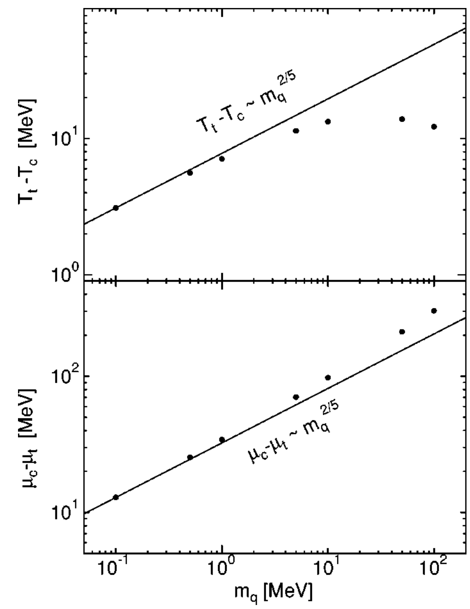

FIG. 4. The quark mass dependence of the critical temperature (upper figure) and the critical chemical potential (lower figure). The slope of the solid line is $\frac{2}{5}$.

$$\chi_q=-\frac{\partial^2\tilde{V}[\sigma_0]}{\partial\mu^2}. \tag{3.7}$$

Figures 5 and 6 show the results in the chiral limit. As we can see, χ_q is suppressed far below the chiral phase transition line and is enhanced near the TCP. In the chirally symmetric phase, χ_q is equal to the value of the massless free quark gas $\chi_q^{\rm free}$ in this model. The region where χ_q is enhanced is elongated in the direction parallel to the first-order phase transition line. This is because the critical exponent for this direction $(\gamma_q=1)$ is larger than for other directions $(\gamma_q=\frac{1}{2})$. We also find a jump in χ_q along the second-order phase transition line. Inside the critical region, however, the jump must be replaced by a *cusp* with certain critical expo-

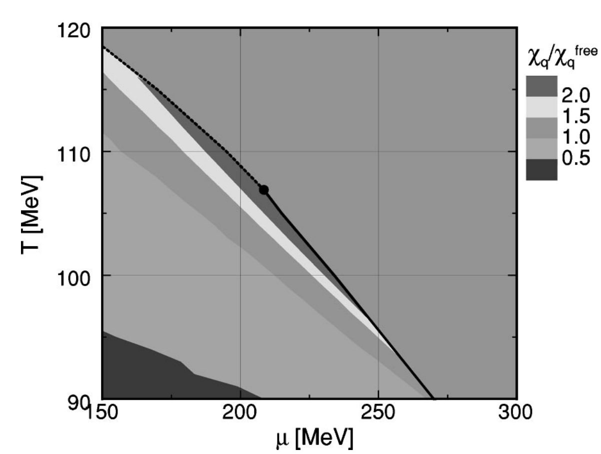

FIG. 5. The quark number susceptibility near the tricritical point in the chiral limit. The value of the susceptibility is divided by that of the massless free quark gas. The solid and dotted lines represent the first- and the second-order phase transitions, respectively, and the filled circle is the tricritical point.

[10]However, we replace p_4 with ω_n, not $\omega_n+i\mu$ in the gauge coupling (3.2) to avoid an absurd situation.

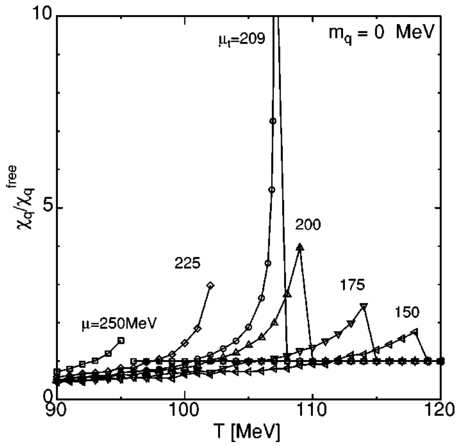

FIG. 6. The temperature dependence of χ_q at fixed μ's. For $\mu<209$ MeV, χ_q has a jump across the second-order phase transition line [$O(4)$ line], which is consistent with the mean field theory. See Appendix B.

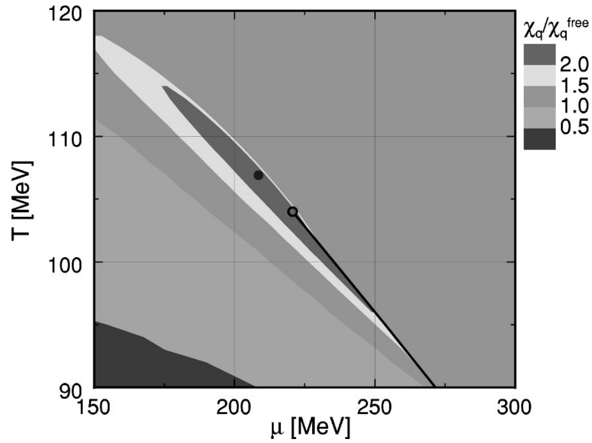

FIG. 7. The quark number susceptibility for $m_q=0.1$ MeV. The value of the susceptibility is divided by that of the massless free theory. The solid line is the first-order transition line. The open circle represents the critical end point for $m_q=0.1$ MeV. The filled circle is at (T_t,μ_t).

nents. See Appendix B. Our model can produce only the mean field behaviors.

Next we examine χ_q for finite quark masses. Figures 7 and 8 are the results for $m_q=0.1$ MeV and $m_q=5.0$ MeV, respectively. The location of the CEP is (T_c,μ_c) $=(104$ MeV, 221 MeV$)$ for $m_q=0.1$ MeV and (95 MeV, 279 MeV) for $m_q=5.0$ MeV. χ_q diverges at the CEP and is enhanced in the elongated region parallel to the first-order phase transition line because the critical exponent is the largest for this direction as in the massless case. For $m_q=0.1$ MeV, the TCP is still close to the CEP and the elongated region includes the point (T_t,μ_t) while for $m_q=5.0$ MeV, the region deviates from it.

At first sight, one might think that the analysis made in the previous section ceases to be valid at somewhere between $m_q=0.1$ MeV and $m_q=5$ MeV and the effect of the TCP no longer survives for $m_q=5$ MeV, which might be considered as the ''realistic'' quark mass in this model.[11] However, this conclusion is too hasty. We will see in the next section that the hidden tricritical point still affects the physics near the CEP even for $m_q=5$ MeV.

C. The critical exponent for χ_q

Now let us examine the critical exponent for χ_q at the CEP and TCP. We calculate it along the path parallel to the μ axis in the T-μ plane from lower μ towards the CEP or TCP at fixed T_c or T_t.

First we consider the chiral limit. We expand $\tilde{V}$ in the vicinity of the TCP:[12]

$$\tilde{V}[\sigma,m_q=0]=V_{\rm free}+a_2(T,\mu)\sigma^2+a_4(T,\mu)\sigma^4+a_6(T,\mu)\sigma^6. \tag{3.8}$$

The coefficients a_2,a_4,a_6, and $V_{\rm free}$ are summarized in Appendix A. σ_0 is determined by the equation $\partial\tilde{V}/\partial\sigma|_{\sigma=\sigma_0}=0$. We obtain

$$\tilde{V}[\sigma_0=0,m_q=0]=V_{\rm free} \tag{3.9}$$

above the chiral transition line, and

$$\tilde{V}[\sigma_0,m_q=0]=V_{\rm free}+\frac{a_4}{27a_6^2}(2a_4^2-9a_2a_6)-\frac{2}{27a_6^2}(a_4^2-3a_2a_6)^{3/2} \tag{3.10}$$

below that line. χ_q is obtained by taking the second derivative of Eqs. (3.9) and (3.10) with respect to μ. Figure 9 shows χ_q for numbers of $|\mu-\mu_t|$'s. We determine the critical exponent γ_q defined in Eq. (2.14) numerically by using a linear logarithmic fitting

$$\ln\chi_q=-\gamma_q\ln|\mu-\mu_t|+{\rm const}, \tag{3.11}$$

where const is independent of μ. We obtain $\gamma_q=0.51\pm0.01$, which is consistent with the mean field theory.

With finite quark masses, the expectation value σ_0 is determined only numerically. This time we do not expand the potential around σ_0 and directly read the exponent from Figs. 7 and 8. In Fig. 10, χ_q is plotted for numbers of $|\mu-\mu_c|$'s for $m_q=0.1$, 5, and 100 MeV together with the calculated values of the critical exponent ϵ defined in Eq. (2.9):

$$\ln\chi_q=-\epsilon\ln|\mu-\mu_c|+{\rm const}. \tag{3.12}$$

For $m_q=0.1$ MeV we obtained ϵ=0.55±0.02. This is significantly different from the prediction of the mean field theory $\epsilon=\frac{2}{3}$, which is clear evidence of the effect of the

[11]In this model $\langle\bar{q}q\rangle_{\Lambda=1\ \rm GeV}=(-276\ \rm MeV)^3$ at $T=\mu=0$. By using Gell-Mann–Oakes–Renner relation with $m_\pi=140$ MeV, $m_q^{\Lambda=1\ \rm GeV}\sim4$ MeV.

[12]The reason for this expansion is twofold. First, in order to keep in line with the argument given in Sec. II. Second, technically we can approach the TCP much closer to determine the exponent than directly reading it from Fig. 5.

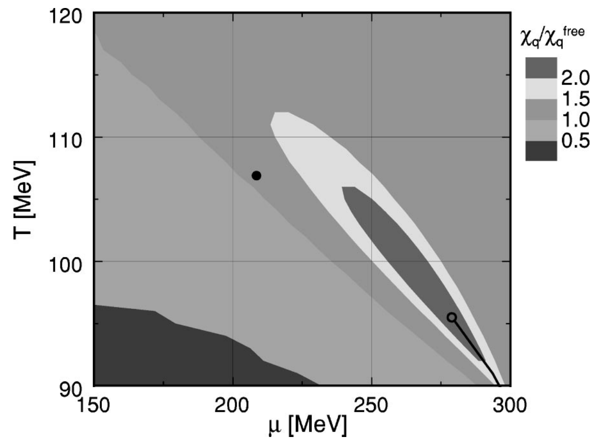

FIG. 8. The quark number susceptibility for $m_q = 5$ MeV. The value of the susceptibility is divided by that of the massless free theory. The open circle is the critical end point for $m_q = 5$ MeV and the filled circle is at (T_t, μ_t).

tricritical point. We expect that the exponent changes towards $\frac{2}{3}$ if we approach the CEP much closer.

For $m_q = 5$ MeV, the slope of the data points changes at around $|\mu - \mu_c| \sim 0.5$ MeV. Therefore we fitted the data for $|\mu - \mu_c| < 0.3$ MeV and >1 MeV separately and obtained the critical exponent 0.68 ± 0.02 for $|\mu - \mu_c| < 0.3$ MeV and 0.57 ± 0.01 for $|\mu - \mu_c| > 1$ MeV. We interpret this change of the exponent as the *crossover* of different universality classes discussed in the previous section. Note that the purely mean-field-like exponent is seen in a very small region $|\mu - \mu_c| < 1$ MeV from the CEP. This result is somewhat surprising to the present authors because, as seen in Fig. 8, the TCP is far away from the CEP already for $m_q = 5$ MeV and the value of χ_q itself is unremarkable at (T_t, μ_t). It seems that, although the analysis in the previous section was made in the small quark mass limit, the effect of the TCP is unexpectedly robust against the increase of the quark mass.

As a check, we also calculated the exponent for $m_q = 100$ MeV and obtained $\epsilon = 0.64 \pm 0.03$ which is consistent with the mean field value $\frac{2}{3}$. For such a large quark mass, we

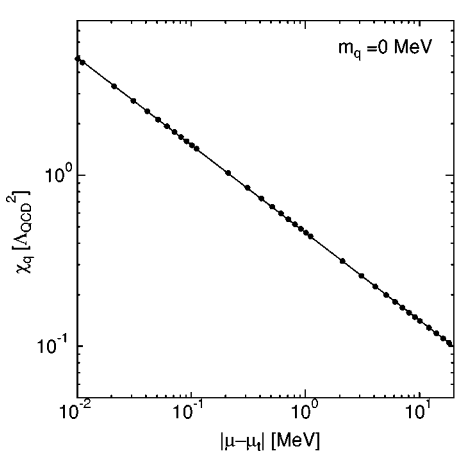

FIG. 9. The quark number susceptibility in the chiral limit as a function of $|\mu - \mu_t|$ at fixed temperature T_t.

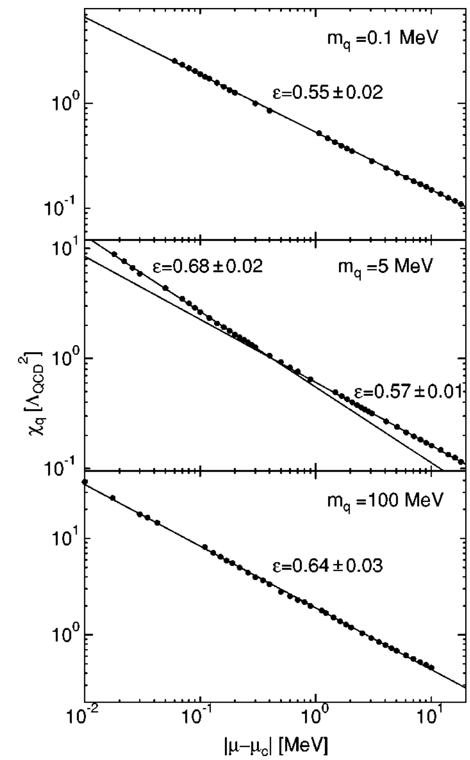

FIG. 10. The quark number susceptibility for $m_q = 0.1$, 5, and 100 MeV as a function of $|\mu - \mu_c|$ at fixed temperature $T_c(m_q)$.

see no indication of a change in the slope. The effect of the TCP has completely disappeared.

IV. CONCLUSIONS

Based on the universality argument and numerical model calculations, we studied the singular behavior of susceptibilities near the critical or tricritical points. These two approaches are complementary, and we observed that the model calculation faithfully quantified the qualitative predictions obtained by using the universality argument as long as the mean field behaviors are concerned. The important point is that, although we adopted a specific model, the qualitative behavior of χ_q is probably model independent. In particular, our results strongly suggest a possibility that the tricritical point affects the physics near the critical end point. In other words, there are *traces* of the hidden tricritical point on the QCD phase diagram. Practically, the traces will be seen as the gradual change of the critical exponents since, after all, universality classes are characterized only by their critical exponents. It is expected that the exponents change from those of the TCP to those of the Ising model via those of the CEP in the mean field approximation. In order to really confirm this fascinating possibility, lattice simulations at finite chemical potentials [39] are necessary.

Finally, we briefly comment on the implication of our results on heavy-ion experiments. The divergence of χ_q is directly related to an anomaly in the event-by-event fluctuation of baryon number B (divided by the entropy S)

$$\frac{\langle (\Delta B)^2 \rangle}{S}, \tag{4.1}$$

which was originally introduced in [21] to probe the deconfined phase. Although neutrons are not observed, we expect that the event-by-event fluctuation of the *proton number* is relatively enhanced for collisions which have passed ''near'' the CEP or the TCP. Pion and diphoton observables are discussed in [12–14]. As we remarked before, the critical exponents of the Ising model and the mean field theory are not so different numerically. Thus, the smallness of the critical region itself may not be an obstacle in the observability of critical phenomena in experiments. However, if we take the effect of the TCP seriously either by assumption or stimulated by future lattice results, we must take into account the long-wavelength fluctuations of the *pions* as well as the sigma meson because the pions are no longer the ''environment'' but participate in the critical fluctuations around the trace of the TCP.

ACKNOWLEDGMENTS

We greatly thank T. Hatsuda and T. Kunihiro for their continuous encouragement and numerous valuable discussions. We also thank M. Asakawa, K. Itakura, L. McLerran, R.D. Pisarski, and M.A. Stephanov for discussions and comments. T.I. is supported by Special Postdoctoral Researchers Program of RIKEN. Y.H. acknowledges RIKEN BNL Research Center where this work was completed.

APPENDIX A: DESCRIPTION OF THE MODEL

1. The normalized CJT effective potential

We begin with the Cornwall-Jackiw-Tomboulis (CJT) effective potential [25] for QCD in the improved-ladder approximation [10] as a functional of the quark propagator $S(p)$ at zero temperature and quark chemical potential after the Wick rotation,

$$V[S]=V_1[S]+V_2[S], \tag{A1}$$

$$V_1[S]=\int \frac{d^4p}{(2\pi)^4}\mathrm{tr}\{\ln[S_0^{-1}(p)S(p)]-S_0^{-1}(p)S(p)+1\}, \tag{A2}$$

$$V_2[S]=-\frac{1}{2}\int\int\frac{d^4p}{(2\pi)^4}\frac{d^4k}{(2\pi)^4}g^2(p-k)\times\left\{\mathrm{tr}\left[\frac{\lambda^a}{2}\gamma_\mu S(k)\frac{\lambda^a}{2}\gamma_\nu S(p)\right]D_{\mu\nu}(p-k)\right\}. \tag{A3}$$

Here ''tr'' is taken over the Dirac, flavor and color matrices (Gell-Mann matrices λ^a), and $S_0(p)$ and $D_{\mu\nu}(p-k)$ are the free quark propagator and the gluon propagator in the Landau gauge $[D_{\mu\nu}(p-k)=(\delta_{\mu\nu}-p_\mu p_\nu/p^2)/p^2]$, respectively. $V_1[S]$ corresponds to the 1-loop potential with the quark 1-loop diagram and $V_2[S]$ is the 2-loop potential with the one gluon exchange.

We adopt the so-called Higashijima-Miransky approximation [40,41] for the QCD running coupling constant

$$g^2((p-k)^2)\to\theta(p^2-k^2)\overline{g^2}(p^2)+\theta(k^2-p^2)\overline{g^2}(k^2), \tag{A4}$$

where $\overline{g}$ is defined in Eq. (3.2). In this approximation with the Landau gauge, the renormalization of the quark wave function may be neglected at zero temperature and chemical potential. At finite temperature and chemical potential we need to take the wave function renormalization into account even in the Landau gauge [42]. However, we ignore this problem for the present purpose. Then the CJT effective potential can be rewritten as Eq. (3.1) in terms of the dynamical quark mass function $\Sigma(p)$ using the corresponding Schwinger-Dyson equation for $\Sigma(p)$.

As a normalization, we define $\tilde{V}$ by subtracting the σ-independent part from V such that $\tilde{V}$ reduces to the value of the free quark gas when $\sigma=0$. We obtain

$$\begin{aligned}\tilde{V}[\sigma,m_q]=&V_{\rm free}-\frac{T}{\pi^2}\sum_{n=0}^{\infty}\int_0^\infty d|\boldsymbol{p}|\boldsymbol{p}^2\ln\frac{[\Sigma^2(\boldsymbol{p}^2,\omega_n^2;\sigma,m_q)+\boldsymbol{p}^2+\omega_n^2-\mu^2]^2+4\mu^2\omega_n^2}{[\Sigma^2(\boldsymbol{p}^2,\omega_n^2;0,m_q)+\boldsymbol{p}^2+\omega_n^2-\mu^2]^2+4\mu^2\omega_n^2}\\&+\frac{16T}{3C_Fa\pi^2}\sum_{n=0}^{\infty}\int_0^\infty d|\boldsymbol{p}|\boldsymbol{p}^2\frac{(\boldsymbol{p}^2+\omega_n^2)(\boldsymbol{p}^2+\omega_n^2+p_c^2)[\ln(\boldsymbol{p}^2+\omega_n^2+p_c^2)]^2}{(\boldsymbol{p}^2+\omega_n^2+p_c^2)\ln(\boldsymbol{p}^2+\omega_n^2+p_c^2)+\boldsymbol{p}^2+\omega_n^2}\left(m_qa\sigma\frac{[\ln(\boldsymbol{p}^2+\omega_n^2+p_c^2)]^{-2}}{(\boldsymbol{p}^2+\omega_n^2+p_c^2)^3}\right.\\&\left.\times\left[\ln(\boldsymbol{p}^2+\omega_n^2+p_c^2)+1-\frac{a}{2}\right]-\frac{\sigma^2}{(\boldsymbol{p}^2+\omega_n^2+p_c^2)^4}[\ln(\boldsymbol{p}^2+\omega_n^2+p_c^2)]^{a-4}\left[\ln(\boldsymbol{p}^2+\omega_n^2+p_c^2)+1-\frac{a}{2}\right]^2\right),\end{aligned} \tag{A5}$$

where $a=24/(11N_c-2N_f)$ and the effective potential for the free quark $V_{\rm free}$ is given by

$$V_{\rm free}=-2T\int\frac{d^3\boldsymbol{p}}{(2\pi)^3}[\ln(1+e^{-(\omega-\mu)/T})+\ln(1+e^{-(\omega+\mu)/T})] \tag{A6}$$

with $\omega=\sqrt{\boldsymbol{p}^2+m_q^2}$. In the chiral limit $(m_q=0)$, the momentum integral can be easily performed and $V_{\rm free}$ becomes

$$V_{\rm free}(m_q=0)=-\left(\frac{\mu^4}{12\pi^2}+\frac{\mu^2T^2}{6}+\frac{7\pi^2T^4}{180}\right). \tag{A7}$$

The quark number susceptibility of the massless free quark gas is given by (omitting the overall factor $N_f N_c$)

$$\chi_q^{\rm free}(m_q=0)=\frac{T^2}{3}+\frac{\mu^2}{\pi^2}. \tag{A8}$$

2. The pion decay constant in the Pagels-Stokar formula

The parameters p_c and $\Lambda_{\rm QCD}$ are determined such that they reproduce the pion decay constant $f_\pi=93$ MeV in the chiral limit. We calculate f_π by the Pagels-Stokar formula [37]

$$f_\pi^2=4N_c\int\frac{d^4p}{(2\pi)^4}\frac{\Sigma[p;\sigma_0,m_q=0)}{[\Sigma^2(p;\sigma_0,m_q=0)+p^2]^2}\times\left[\Sigma(p;\sigma_0,m_q=0)-\frac{p^2}{2}\frac{d\Sigma(p;\sigma_0,m_q=0)}{dp^2}\right]. \tag{A9}$$

In the above equation, we set $N_f=2$ because the pion consists of u and d quarks.

3. Coefficients in the mean field expansion

The explicit expressions of the coefficients a_2, a_4 and a_6 in Eq. (3.8) are

$$a_2(T,\mu)=\frac{1}{\pi^2}T\sum_{n=0}^{\infty}\int d|\boldsymbol{p}|\boldsymbol{p}^2\left\{-\frac{2[\ln(\boldsymbol{p}^2+\omega_n^2+p_c^2)]^{a-2}(\boldsymbol{p}^2+\omega_n^2-\mu^2)}{(\boldsymbol{p}^2+\omega_n^2+p_c^2)^2[(\boldsymbol{p}^2+\omega_n^2-\mu^2)^2+4\mu^2\omega_n^2]}+\frac{9}{2}\frac{\left[\ln(\boldsymbol{p}^2+\omega_n^2+p_c^2)+1-\frac{a}{2}\right]^2(\boldsymbol{p}^2+\omega_n^2)[\ln(\boldsymbol{p}^2+\omega_n^2+p_c^2)]^{a-2}}{(\boldsymbol{p}^2+\omega_n^2+p_c^2)[(\boldsymbol{p}^2+\omega_n^2+p_c^2)\ln(\boldsymbol{p}^2+\omega_n^2+p_c^2)+\boldsymbol{p}^2+\omega_n^2]}\right\}, \tag{A10}$$

$$a_4(T,\mu)=\frac{1}{\pi^2}T\sum_{n=0}^{\infty}\int d|\boldsymbol{p}|\boldsymbol{p}^2\frac{[\ln(\boldsymbol{p}^2+\omega_n^2+p_c^2)]^{2a-4}[(\boldsymbol{p}^2+\omega_n^2-\mu^2)^2-4\mu^2\omega_n^2]}{(\boldsymbol{p}^2+\omega_n^2+p_c^2)^4[(\boldsymbol{p}^2+\omega_n^2-\mu^2)^2+4\mu^2\omega_n^2]^2}, \tag{A11}$$

$$a_6(T,\mu)=-\frac{2}{3\pi^2}T\sum_{n=0}^{\infty}\int d|\boldsymbol{p}|\boldsymbol{p}^2\frac{[\ln(\boldsymbol{p}^2+\omega_n^2+p_c^2)]^{3a-6}(\boldsymbol{p}^2+\omega_n^2-\mu^2)[(\boldsymbol{p}^2+\omega_n^2-\mu^2)^2-12\mu^2\omega_n^2]}{(\boldsymbol{p}^2+\omega_n^2+p_c^2)^6[(\boldsymbol{p}^2+\omega_n^2-\mu^2)^2+4\mu^2\omega_n^2]^3}. \tag{A12}$$

APPENDIX B: THE $O(4)$ CRITICAL LINE

In this appendix, for completeness, we examine the singular behavior of χ_q along the $O(4)$ line emerging from the TCP toward the temperature axis in the $m=0$ plane (see, Fig. 1). We call this line the $O(4)$ line because it consists of a sequence of critical points whose universality class is the same as that of the $O(4)$ spin model [2]. We again start with (2.1) with $m=0$ and the replacement $\sigma^2\to\phi^2\equiv\sigma^2+(\pi^1)^2+(\pi^2)^2+(\pi^3)^2$. The $O(4)$ line in the (T,μ) plane is determined by the following equation:

$$a(T,\mu)=0. \tag{B1}$$

Since $b>0$ does not vanish and smoothly varies along this line, we can drop the ϕ^6 term. If we consider the mean field behavior, we can expand a around an arbitrary point (T_c,μ_c) on the line [30]

$$a(T,\mu)=C'(T-T_c)+D'(\mu-\mu_c). \tag{B2}$$

In the mean field approximation, the (singular part of) thermodynamic potential becomes

$$\Omega_{MF}=0 \tag{B3}$$

above the $O(4)$ line, and

$$\Omega_{MF}=-\frac{a^2}{4b} \tag{B4}$$

below the $O(4)$ line. Taking the second derivative in μ, we see that the quark number susceptibility has a discontinuous jump across (T_c,μ_c) and that it is larger in the low temperature phase [below the $O(4)$ line] than in the high temperature phase [above the $O(4)$ line] except for points where $D'=0$. Beyond the mean field approximation, we use the current theoretical estimate of the specific heat exponent of the $O(4)$ spin model [43]

$$\alpha\sim-0.2. \tag{B5}$$

The minus sign means that the quark number susceptibility shows a cusp at T_c as in the case of the λ point of liquid helium. [α is also negative for the $O(2)$ model.] Note that $(T_c,\mu=0)$ is the point where $D'=0$. It was shown in [44] that the $O(4)$ line is perpendicular to the temperature axis.

Thus the quark number susceptibility has no singularity at $(T_c, \mu=0)$ even in the chiral limit and increases monotonically as a function of the temperature, consistent with the results of lattice simulations. However, this smooth behavior is an exception only at $\mu=0$. At any nonzero μ, χ_q has a cusp precisely at the critical temperature $T_c(\mu)$. The cusp becomes higher and higher as we increase μ and finally diverges at the tricritical point.

[1] See, for example, H. Satz, Nucl. Phys. **A681**, 3 (2001); **A661**, 104 (1999).
[2] R.D. Pisarski and F. Wilczek, Phys. Rev. D **29**, 338 (1984).
[3] M. Asakawa and K. Yazaki, Nucl. Phys. **A504**, 668 (1989).
[4] M.A. Halasz, A.D. Jackson, R.E. Shrock, M.A. Stephanov, and J.J. Verbaarschot, Phys. Rev. D **58**, 096007 (1998).
[5] J. Berges and K. Rajagopal, Nucl. Phys. **B538**, 215 (1999).
[6] M. Harada and A. Shibata, Phys. Rev. D **59**, 014010 (1999).
[7] S.P. Klevansky, Rev. Mod. Phys. **64**, 649 (1992).
[8] A. Barducci, R. Casalbuoni, G. Pettini, and R. Gatto, Phys. Rev. D **49**, 426 (1994); A. Barducci, R. Casalbuoni, S. de Curtis, R. Gatto, and G. Pettini, Phys. Lett. B **231**, 463 (1989); Phys. Rev. D **42**, 1757 (1990).
[9] M.G. Alford, K. Rajagopal, and F. Wilczek, Phys. Lett. B **422**, 247 (1998).
[10] O. Kiriyama, M. Maruyama, and F. Takagi, Phys. Rev. D **62**, 105008 (2000); **63**, 116009 (2001).
[11] Z. Fodor and S.D. Katz, Phys. Lett. B **534**, 87 (2002); J. High Energy Phys. **03**, 014 (2002).
[12] M. Stephanov, K. Rajagopal, and E. Shuryak, Phys. Rev. Lett. **81**, 4816 (1998); Phys. Rev. D **60**, 114028 (1999).
[13] B. Berdnikov and K. Rajagopal, Phys. Rev. D **61**, 105017 (2000).
[14] K. Fukushima, hep-ph/0209270.
[15] V.L. Ginzburg, Sov. Phys. Solid State **2**, 1824 (1960).
[16] M. Ley-Koo and M.S. Green, Phys. Rev. A **16**, 2483 (1977).
[17] F.J. Wegner, Phys. Rev. B **5**, 4529 (1972).
[18] L.D. McLerran, Phys. Rev. D **36**, 3291 (1987).
[19] T. Kunihiro, Phys. Lett. B **271**, 395 (1991).
[20] A. Gocksch, Phys. Rev. Lett. **67**, 1701 (1991).
[21] M. Asakawa, U. Heinz, and B. Müller, Phys. Rev. Lett. **85**, 2072 (2000).
[22] S. Gottlieb, W. Liu, D. Toussaint, R.L. Renken, and R.L. Sugar, Phys. Rev. Lett. **59**, 2247 (1987); Phys. Rev. D **38**, 2888 (1988).
[23] R.V. Gavai, J. Potvin, and S. Sanielevici, Phys. Rev. D **40**, 2743 (1989).
[24] R.V. Gavai and S. Gupta, Phys. Rev. D **64**, 074506 (2001).
[25] J.M. Cornwall, R. Jackiw, and E. Tomboulis, Phys. Rev. D **10**, 2428 (1974).
[26] O. Kiriyama, hep-ph/0112106.
[27] See, for example, S. K. Ma, *Modern Theory of Critical Phenomena* (Perseus Publishing, Cambridge, MA, 1976).
[28] See, for example, J. Hubbard and P. Schofield, Phys. Lett. **40A**, 245 (1972).
[29] For a review, see I. Lawrie, and S. Sarbach, in *Phase Transitions and Critical Phenomena*, edited by C. Domb and J. Lebowitz (Academic Press, New York, 1984), Vol. 9, p. 1.
[30] This is valid only in the framework of the mean field theory.
[31] R.B. Griffiths and J.C. Wheeler, Phys. Rev. A **2**, 1047 (1970).
[32] B. Widom, J. Chem. Phys. **43**, 3898 (1965).
[33] J.J. Rehr and N.D. Mermin, Phys. Rev. A **8**, 472 (1973).
[34] See, however, J.B. Kogut, M.A. Stephanov, and C.G. Strouthos, Phys. Rev. D **58**, 096001 (1998). The critical region of the critical points on the $O(4)$ line shrinks as μ increases and vanishes at the tricritical point.
[35] N. Giordano and W.P. Wolf, Phys. Rev. Lett. **39**, 342 (1977).
[36] T. Kugo and M.G. Mitchard, Phys. Lett. B **286**, 355 (1992).
[37] H. Pagels and S. Stokar, Phys. Rev. D **20**, 2947 (1979).
[38] See, for example, M. Le Bellac, *Thermal Field Theory* (Cambridge University Press, Cambridge, England, 1996).
[39] Z. Fodor, hep-lat/0209101.
[40] K. Higashijima, Phys. Lett. **124B**, 257 (1983); Phys. Rev. D **29**, 1228 (1984); Prog. Theor. Phys. Suppl. **104**, 1 (1991); P. Castorina and S-Y. Pi, Phys. Rev. D **31**, 411 (1985).
[41] V.A. Miransky, Sov. J. Nucl. Phys. **38**, 280 (1983).
[42] T. Ikeda, Prog. Theor. Phys. **107**, 403 (2002).
[43] R. Guida and J. Zinn-Justin, cond-mat/9803240, and references therein.
[44] C.R. Allton, S. Ejiri, S.J. Hands, O. Kaczmarek, F. Karsch, E. Laermann, Ch. Schmidt, and L. Scorzato, Phys. Rev. D **66**, 074507 (2002). We thank T. Hatsuda for drawing our attention to this paper.
[45] J.P. Blaizot, E. Iancu, and A. Rebhan, Phys. Lett. B **523**, 143 (2001).